Volume 17, Number 3, 2024. pp. 323-330

Jordan Journal of Physics

ARTICLE

Influence of Applied Discharge Voltage and Gas Flow Rate on Nickel Plasma Jet Parameters Diagnosed by Optical Emission Spectroscopic Technique

Ibrahim K. Abbas

Department of Physics, College of Science, University of Baghdad, 10017, Baghdad, Iraq.

Doi: **https://doi.org/10.47011/17.3.7**

Received on: 07/09/2022; *Accepted on: 28/12/2022*

Abstract: In this work, we measure the plasma parameters by using an AC high-voltage power supply that generates a non-thermal plasma jet system at atmospheric pressure. A nickel (Ni) metal strip, with dimensions of 1.5 × 10 cm^2, was connected to the anode electrode of the AC power supply. This nickel strip was immersed in a flask with a small amount of distilled water positioned below the plasma plume nozzle. Optical emission spectroscopy (OES) was used to diagnose the plasma system at different argon gas flow rates (1-5 L/min) and varying applied voltage values (11-15 kV). It is significant to know the processes accompanying plasma generation to measure their parameters which include the electron temperature (T_e), electron number density (n_e) of the plasma, Debye length (λ_D), and plasma frequency (f_p). Our results showed an increase in the intensity of spectral lines with the increase in applied discharge voltage (11-15 kV). The maximum peak for ArI was observed at a wavelength of 811.531 nm, and the maximum peaks for nickel (Ni) were observed at wavelengths of 285.21 and 519.70 nm. Also, the results indicated a gradual increase in electron temperature (T_e) and electron density (n_e) values at the applied voltage of 0.403-0.468 eV. Likewise, the electron density (n_e) was in the range of (11.486-13.851) × 10^{17} cm^{-3}.

Keywords: Atmospheric plasma jet, Nickel (Ni) plasma parameters, Electron temperature, Spectroscopic optical emission (OES).

1. Introduction

Plasma has free-charged particles at the macroscopic level, with both negative and positive charges storing roughly the same amount of energy [1]. The energy needed to generate plasma can be supplied in several ways: through heat from a combustion process, through the interaction between laser radiation and a solid, a liquid, or gas, or through electrical discharges in gases, in which free electrons take energy field and lose it through excitation and ionization processes of the atoms and molecules in the gas. On a macroscopic scale, plasmas are electrically neutral since the number of positive and negative charges is similar [2]. The goal of plasma diagnostics is to obtain information about plasma parameters through various experimental techniques [3]. In order to determine plasma attributes, it is necessary to understand the effects of the numerous physical processes that occur and to determine the effects of these processes. Electrical sampling and optical spectroscopy of emissions are examples of such diagnostics [4]. Spectroscopic procedures, such as laser dispersion, emission, absorption, and fluorescence spectrometry, are unique methods for collecting distinct sections of plasma without altering its status or structure [5]. One of these techniques is optical emission spectroscopy (OES), which relies on calculating the plasma's optical radiation to describe plasma parameters in the chemical, molecular, and ionic radiator's near environments [6, 8]. So, in order to obtain

Corresponding Author: Ibrahim K. Abbas **Email**: Ibrahim.kareem1104a@sc.uobaghdad.edu.iq

information about plasma, such as electron density, excited species state densities, collisional electron–atom, atom-atom, and ion–atom effects, energetic distribution of species, temperature of species, charge transfer between plasma components, rotating structure of molecules, and even electric charge, spectroscopy serves as a non-intrusive method for analyzing electromagnetic radiation from a plasma source [7, 9] Atomic spectra are primarily concerned with the exchange of energy between the atom and electromagnetic radiation, which can be associated with a valence electron changing its orbit in the simplest model [7, 10].

Recent developments have sparked renewed interest in using atmospheric pressure plasmas in a myriad of applications biology, nanotechnology, and agriculture [11]. This is especially true in biomedicine, where uses include inhibiting microorganisms, regenerating tissue, and whitening teeth, among others [12]. For such low-density plasmas, the population densities of the new rates are computed using a balance between radiative decay to ground state and collisional excitations. Due to its ability to recognize and forecast particular properties of plasma, such as populations with particle velocity distribution and relative energy levels, the temperature of the plasma is a crucial thermodynamic attribute. The electron temperature (T_e in eV) is calculated using the equation below [3]:

$$ln\left[\frac{\lambda_{ji}I_{ji}}{hcA_{ji}g_j}\right] = -\frac{1}{K_B T_e}\left(E_j\right) + \ln\left|\frac{N}{U(T)}\right| \quad (1)$$

where g_j denotes the statistical weight of the second spectrum line, λ_{ji} denotes the wavelength of the second level (j) and the first level (i), and E_j is the excited state energy of the upper level. E_i is the first level in the spectrum of plasma in eV, I_{ji} denotes the spectrum intensity of the second level (j) and the first level (i), A_{ji} denotes the transition probability of the second (j) and the first level (i), N denotes the density of the state's population, and K_B denotes the Boltzmann constant. Another main parameter for plasma, the electron density, can be calculated from the equation [3]:

$$n_e = \left[\frac{\Delta\lambda}{2\omega_s}\right] N_r \ (cm^{-3}) \quad (2)$$

where $\Delta\lambda$ is the full width at half maximum (FWHM) in nm of the line, ω_s is the Stark broadening parameter found in standard tables, N_r is the reference electron density. In the analysis of plasma spectra, Stark broadening is an essential factor in spectral line widening because it provides the necessary electron density at the desired plasma electron temperature [13]. Doppler broadening, instrumental broadening, and natural broadening all contribute to the Gaussian profile [14]. If electron impact widening is considered while the ion dynamics are neglected during the radiative process, a Lorentzian profile can be obtained. The frequency of plasma is determined from the following equation [15]:

$$f_p = \sqrt{\frac{e^2 n_e}{\varepsilon_\circ m_e}} = 8.98\sqrt{n_e}\ (\text{Hz}) \quad (3)$$

where e^2 represents electron charge, n_e electron number density, m_e electron mass, and $\varepsilon_\circ$ permittivity. Debye shielding is the response of charged particles to lower local electric fields, giving plasma its quasi-neutrality feature. To calculate the Debye length λ_D, we can use this equation [16]:

$$\lambda_D = \sqrt{\frac{\varepsilon_O K_B T_e}{n_e e^2}} = 743 \times \sqrt{\frac{T_e}{n_e}}\ (cm) \quad (4)$$

The main objective of this paper is to describe the use of OES to analyze a nickel plasma jet, calculate plasma parameters by the Boltzmann plot method, which is used to estimate the electron temperature, calculate other plasma parameters, and understand the effects of increasing applied voltage and gas flow on the behavior of electron temperature and electron density.

2. Material and Methods

2.1. Preparation of Nickel Metal and Main Tools

A small flask containing distilled water was used to partially submerge a nickel-metal (Ni) plate. The detection instrument of the spectrometer was installed close to the plasma jet head to measure the intensity of the emission spectra. An S3000-UV-NIR spectrometer was used to measure the spectral wavelengths emitted during plasma jet generation, with the spectral emission recorded in the range of 270-1000 nm. The dimensions of the nickel plate were 1.5 × 10 cm, with 6 cm of nickel (Ni) submerged in the distilled water. The optical fiber of the spectrometer device sensed the spectral emissions during the generation of the plasma and its interaction with the distilled water

in the flask. The length of the plasma was controlled by the gas flow device (flowmeter) at an applied voltage of 11-15 kV.

2.2. Setup of Plasma Jet System

To generate plasma in this system, argon gas was used. A high alternating voltage power supply of up to 20 kV was used with a cut-off frequency of 50 kHz. The high-voltage power supply represented the main unit in the plasma jet system for ionizing the argon gas and obtaining plasma at room pressure. The cathode electrode of the voltage supply was connected to the tip of the plasma jet, while the anode electrode high-voltage power supply was connected through a connecting wire with nickel metal, which connected with the protruding part of the nickel metal immersed in the flask below the plasma jet as shown in Fig. 1. The voltage used to generate plasma was changed from 11 to 15 kV with the gas flow value fixed at 5 L/min. Similarly, the gas flow rate was varied between 1 and 5 L/min while keeping the applied voltage fixed at 15 kV. Diagnostics were performed in the laboratory at the atmospheric pressure of the room. A spectrometer linked to a control unit (PC) was used to record the resulting spectra and obtain spectral data at the above variables. The plasma spectrum of argon gas was collected at 690-975 nm, while the nickel spectrum data (NiI) was recorded at 280-915 nm. These recorded data were examined and matched with data from the National Institute of Standards and Technology (NIST). Finally, the nickel metal plasma parameters were calculated, and their properties were explained.

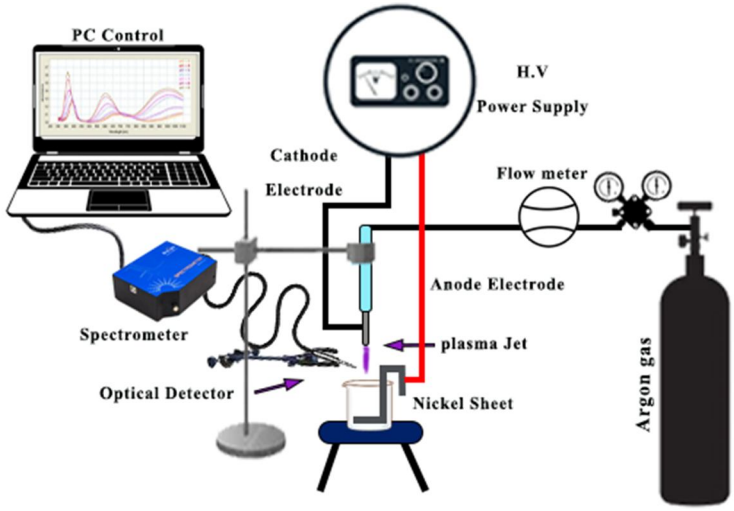

FIG. 1. Schematic setup of atmospheric nickel plasma jet and spectroscopic device with the rest of the tools, including the high voltage power supply to generate plasma, argon gas bottle, and gas flow device controlled by a flowmeter.

3. Results and Discussion

After preparing the plasma system for optical diagnostics, the S3000-UV-NIR optical diagnostic device was prepared, and its optical fiber detector was positioned close to the generated plasma plume. An optical spectrum of the system was obtained using the spectrometer diagnostic device. Figure 2 presents the optical emission spectrum for the plasma jet system at different voltages with a fixed value of argon gas flow. Figure 3 presents the measured optical spectrum for the plasma system at a different flow of argon gas, with the applied voltage fixed at 15 kV.

In both figures, the influence of applied voltage and gas flow on the optical diagnosis is evident, as the peak intensities increase progressively with both factors. The peaks of nitrogen gas (N_2I) appear in the wavelength range of 280 to 422 nm, while the peaks of argon gas (ArI) are observed from 690 to 975 nm. In both figures, the highest peak of nitrogen gas (N_2I) is at a wavelength of 336.93 nm, and the highest peak of argon gas is at 811.53 nm. It is also clear from the figures that multiple peaks of nickel metal NiI are visible from 285 to 915 nm, including peaks at 285.21, 317.39, 335.62, and 409.55 nm, and so on, up to 915.34 nm. These peaks become more pronounced with the

increasing values of influencing factors, indicating a rise in the number of interactions between plasma particles and an increase in the emission of ArI gas. All the peaks illustrated in the two figures correspond to the data from the National Institute of Standards and Technology (NIST) and are consistent with the results of previous studies by other researchers [17-19].

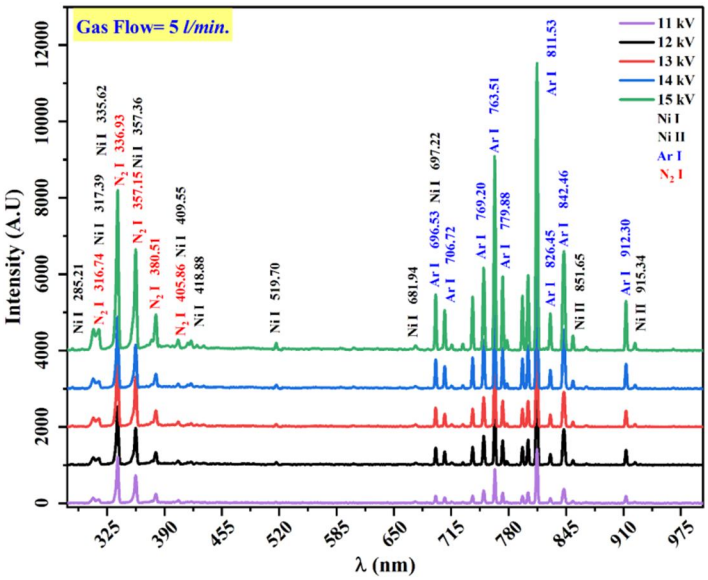

FIG. 2. Diagnosed optical spectrum of a nickel plasma jet system using OES at different discharge voltages (11-15 kV) with a fixed gas flow rate of 5 L/min. The spectrum lines include nickel (Ni), (Ar), and (N_2), ranging from 285.21 to 915.34 nm.

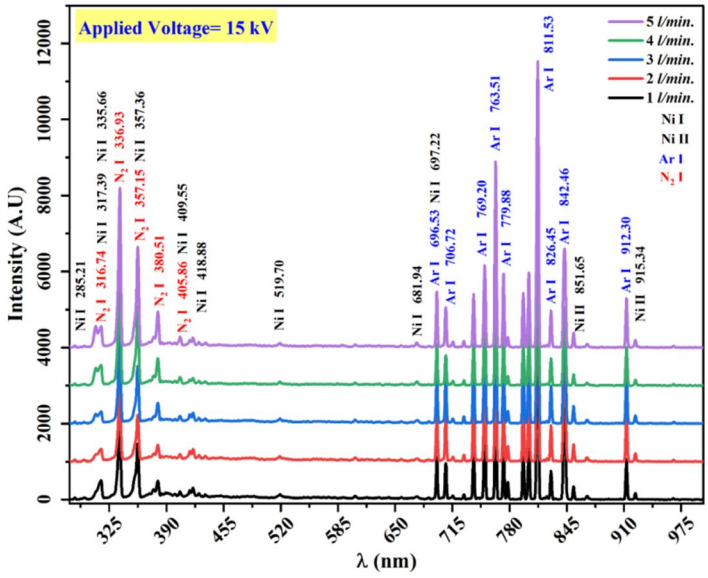

FIG. 3. Diagnosed optical spectrum of a nickel plasma jet system using OES at different gas flow rates (1-5 L/min) with a constant discharge voltage of 15 kV. The spectrum lines include nickel (Ni), (Ar), and (N_2), ranging from 285.21 to 915.34 nm.

At a low flow level of argon gas, a small part of the gas atoms emerging from the plasma nozzle ionizes through interactions and thermal collisions between the atoms. With the gradual increase in the level of gas flow (1-5 L/min) or applied voltage (11-15 kV), and as a result of the applied voltage difference between the electrodes, electrons are released from the negative electrode and are then accelerated. This process, coupled with an increase in the level of gas flow or an increase in the voltage applied, leads to an increase in the collisions of gas atoms. These collisions generate pairs of electrons and ions by interacting with neutral atoms, causing further ionization for these neutral atoms. Nickel metal, which contains secondary electrons on its surface, contributes to the chain of reactions inside the flask, with the increasing flow of argon gas and applied voltage used to generate plasma during diagnostics.

One of the most important parameters of plasma is the electron temperature. Using Eq. (1), one can calculate the temperature by determining the slope of the linear fit of the curve obtained from plotting $ln[\lambda_{ji}I_{ji}/hcA_{ji}g_j]$ versus E_j, as shown in Fig. 4. Another important plasma parameter is the electron number density (ne), which can be determined through the data obtained by using Eq. (2). This calculation involves the full width at half maximum (FWHM) values at each applied voltage (11-15 kV), as shown in Fig. 5.

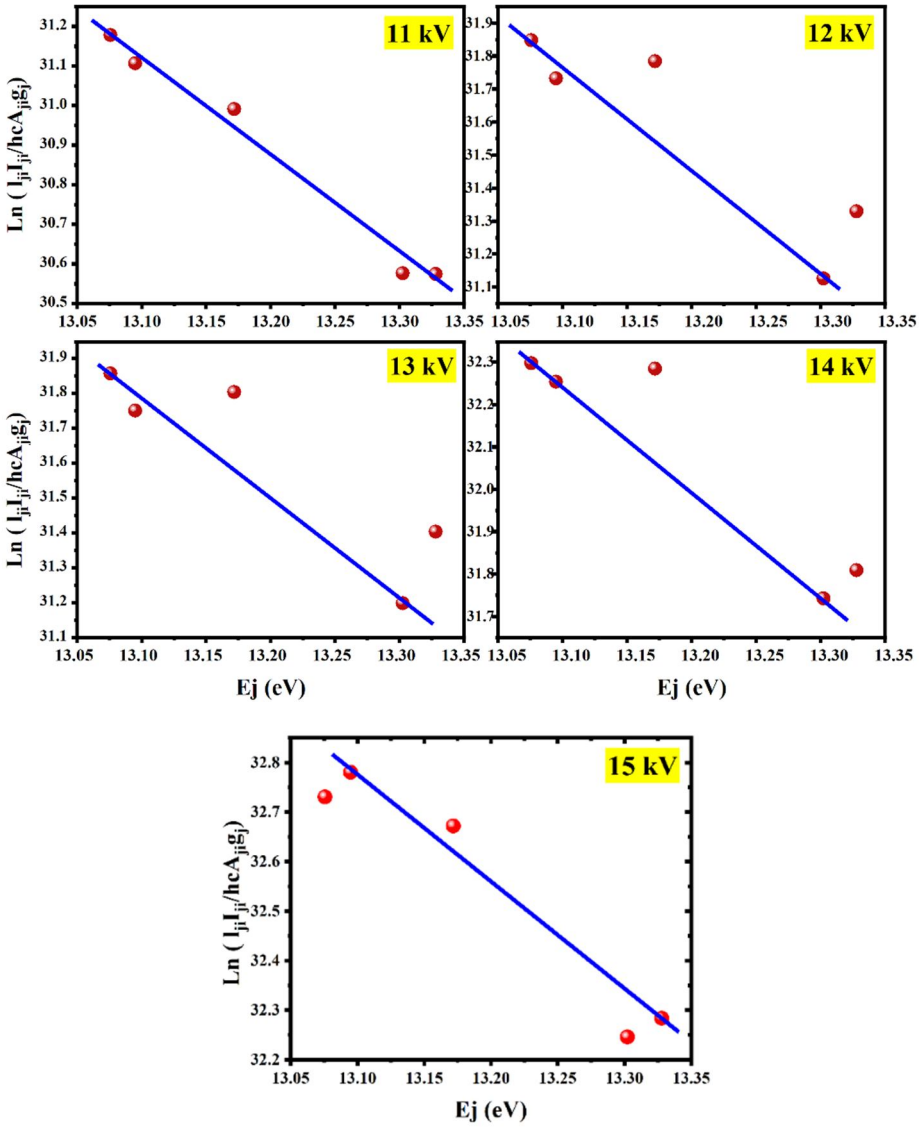

FIG. 4. Boltzmann plot of $ln[\lambda_{ji}I_{ji}/hcA_{ji}g_j]$ vs. the upper energy level (E_j) of nickel metal spectrum generated by an atmospheric plasma jet system for different values of applied voltage (11-15 kV) and constant gas flow rate of 5 L/min.

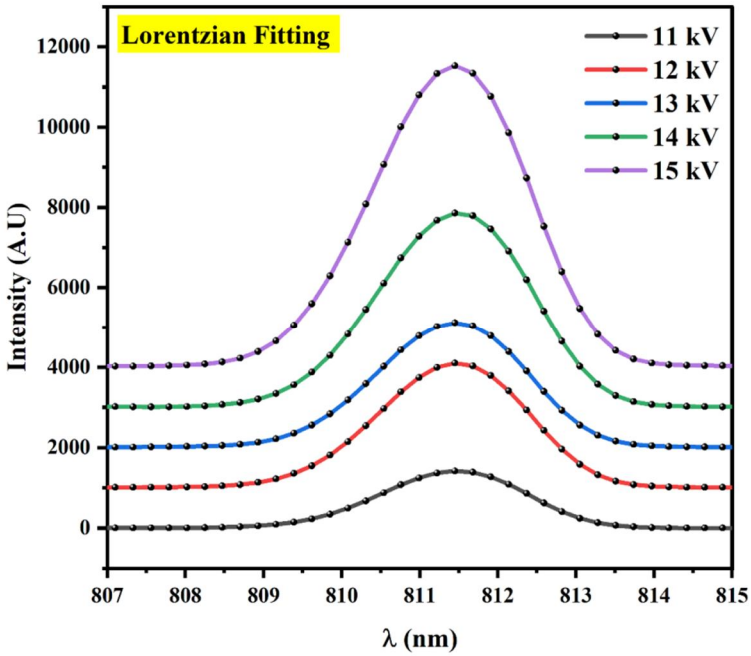

FİG. 5. Full width at half maximum (FWHM) of the nickel metal spectrum in an atmospheric plasma jet system at different values of applied voltage (11-15 kV) and a constant gas flow rate of 5 L/min (Lorentzian Fitting) at 807-815 nm.

Table 1 shows the measured plasma parameters diagnosed at a variable applied voltage of 11-15 kV, with the gas flow value being fixed at 5 L/min. These plasma jet parameters were determined using Eqs. (1) - (4). It is clear from the table that the measured plasma frequency f_p increases with the increase in the applied voltage values, while the Debye length λ_D decreases with the increase in the applied voltage under the same argon gas flow conditions.

TABLE 1. Atmospheric plasma jet parameters for nickel metal (Ni) at different applied voltages (11-15 kV) with a fixed gas flow rate of 5 L/min.

V (kV)	Te (ev)	FWHM (nm)	ne x 10^{17} (cm^{-3})	f_p x 10^{12} (Hz)	λ_D (x 10^{-6} cm)
11	0.403	1.700	11.486	9.624	0.440
12	0.427	1.800	12.162	9.903	0.428
13	0.451	1.900	12.838	10.175	0.441
14	0.448	2.000	13.514	10.439	0.430
15	0.468	2.050	13.851	10.569	0.432

Figure 6 depicts the correlation between electron temperature and electron number density as a function of the applied voltage used to generate plasma in this system. The results show a clear increase in electron temperature from 0.403 to 0.468 eV with increasing applied voltage at a constant argon gas flow rate of 5 L/min. Similarly, the electron density increases from 11.486 x 10^{17} to 13.851 x 10^{17} cm^{-3} at an applied voltage of 11-15 kV. At the first value of the applied voltage, 11 kV, the electron temperature was 0.403 eV and the electron density was 11.486 x 10^{17} cm^{-3}. With the increased value of the applied voltage, electron temperature and density began to rise. The reason for this is the increase in the neutral electronic collisions that occur on the walls of the plasma jet. The value of the electron temperature at 15 kV is 0.468 eV, and the electron density is 13.851x10^{17} cm^{-3}.

There are more collisions between electrons and argon atoms before getting out of the plasma nozzle when the applied voltage is gradually increased, which results in an increase in the amount of energy transferred from electrons to gas molecules, which increases the temperature of the gas, so the electron density will gradually increase, especially since gas flow is 5 L/min.

This behavior indicates that the amount of argon gas passing through the plasma is substantial, leading to a slight increase in both

electron temperature and density. It is clear that the applied voltage is directly related to the measured plasma parameters, as electrons are accelerated from the cathode to the anode, gaining kinetic energy and colliding with gas molecules between the electrodes. This acceleration continues until the electron collides with an argon gas molecule. At lower collision energies, only elastic scattering occurs. However, as the applied voltage increases gradually from 11 kV to 15 kV, electrons can lose significant amounts of energy by exciting gas molecules to higher internal energy states, and at even higher energies, ionization can occur within the plasma jet.

The ionization process is, of course, essential to achieve an increase in electron temperature and number density. Consequently, some of electrons are absorbed by the neutral particles, while others are lost in collisions (electron-neutral particles). The loss of charged particles (electrons and ions) takes place through diffusion to the walls of the plasma jet tube, where they recombine. In the case of the plasma jet, the shape of the plasma tube resembles a cylinder, with ionization and collision events occurring along and inside this cylindrical column. Under these conditions, the tube radius of the plasma jet influences electron distribution through collisions and diffusion to the walls by an increase in applied discharge voltage and argon gas flow [20-22]. As the applied field accelerates the newly liberated and colliding electrons, a secondary ionization process occurs, leading to the collapse process, which increases electron temperature and electron number density in the plasma jet system, as shown in Fig. 6, consistent with previous studies [3,14].

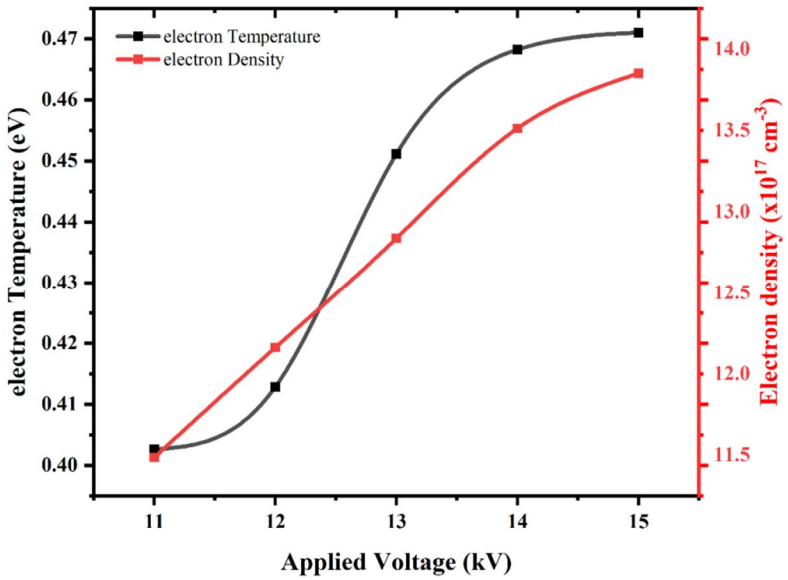

FIG. 6. Electron temperature (T_e) and electron number density (n_e) plot for the nickel metal plasma jet at different applied voltages (11-15 kV) and a constant flow rate of 5 *l/min*. The highest electron temperature (Te = 0.468 eV) and electron number density (n_e=13.851x10^{17} cm^{-3}) were both observed at an appplied voltage of 15 kV.

4. Conclusions

In this research, the results obtained by measuring and studying the plasma parameters of nickel showed a clear discrepancy between electron temperature (T_e) in the plasma and electron number density (n_e) with the gradual increase of applied voltage from 11 to 15 kV during plasma generation. The electron temperature ranged from 0.403 to 0.468 eV, while the electron number density values ranged from 11.486 x 10^{17} to 13.851 x 10^{17} cm^{-3} for the different applied voltages. Many spectral peaks of these emissions were observed as well, including spectral lines for Argon (ArI), (NiI), and (N_2I). The highest intensity for argon gas (ArI) was obtained at a wavelength of 811.53 nm, while the maximum peak for nitrogen gas (N_2I) was found at 336.93 nm. Multiple nickel emission line peaks appeared, ranging from 285.21 to 915.34 nm. According to the results, the rise in spectral emission intensity caused by the passage of argon gas indicates that the number of gas molecules is increasing. This implies that the electrolyte field's energy is

sufficient to induce secondary ionization of molecules, hence ionizing the vast majority of gas particles traveling through the plasma tube. Consequently, this points to a close correlation between the increase in energy and the increase in the values of the measured plasma parameters.

Acknowledgments

I would like to express my gratitude and thanks to the plasma laboratory in the Physics Department, College of Science, University of Baghdad. I would also like to express gratitude to everyone who inspired me to continue on the path of knowledge.

References

[1] Aadim, K.A. and Jassim, R.H., AIP Conference Proceedings, 2372 (2021) 80014.

[2] Khlyustova, A., Labay, C.P., Machala, Z., Ginebra, M.P. and Barnils, C., Front. Chem. Sci. Eng., 13 (2019) 238.

[3] Baniya, H.B., Shrestha, R., Guragain, R.P., Pandey, B.P. and Subedi, D.P., Int. J. Polym. Sci., 2020 (2020) 9247642.

[4] Lu, X., Xiong, Z., Zhao, F., Xian, Y., Xiong, Q., Gong, W., Zou, C., Jiang, Z. and Pan, Y., Appl. Phys. Lett., 95 (2009) 181501.

[5] Adamovich, I., Baalrud, S.D., Bogaerts, A., Bruggeman, P.J. and Cappelli, M., J. Phys. D. Appl. Phys., 50 (2017) 323001.

[6] Suhail, M.H., Adim, K.A. and Wanas, A.H., Br. J. Appl. Sci. Technol., **7** (2015) 263.

[7] Hyde, A. and Batishchev, O., Rev. Sci. Instrum., 91 (2020) 63502.

[8] Akatsuka, H., Adv. Phys. X, 4 (2019) 1592707.

[9] Asenjo-Castillo, J. and Vargas-Blanco, I., Rev. Tecnol. en Marcha., 29 (2016) 47.

[10] Donati, G.L., Amais, R.S. and Williams, C.B., J. Anal. At. Spectrom., 32 (2017) 1283.

[11] Yong, W., Cong, L.I., Jielin, S.H.I., Xingwei, W.U. and Hongbin, D., Plasma Sci. Technol., 19 (2017) 115403.

[12] Chen, Z., Chen, G., Obenchain, R., Zhang, R. and Bai, F., Mater. Today, 54 (2022) 153.

[13] Safeen, A., Shah, W.H., Khan, R., Shakeel, A. and Iqbal, Y., Dig. J. Nanomater. Biostructures, 14 (2019) 29.

[14] Garcia, M.C., Yubero, C. and Rodero, A., Plasma Sources Sci. Technol., 29 (2020) 55006.

[15] Benedikt, J., Kersten, H. and Piel, A., Plasma Sources Sci. Technol., 30 (2021) 33001.

[16] Wu, F., Li, J., Xian, Y., Tan, X. and Lu, X., Plasma Process. Polym., 18 (2021) 2100033.

[17] Aadim, K.A., Iraqi J. Phys., 15 (2018) 117.

[18] Mohammed, R.S., Aadim, K.A. and Ahmed, K.A., AIP Conference Proceedings, 2386 (2022) 80050.

[19] Zaplotnik, R., Primc, G. and Vesel, A., Appl. Sci., 11 (2021) 22.

[20] Michel, A., Jacques, D., Anne, L. and Cédric, D.V., (Springer, 2006) ISBN 978-94-007.

[21] Rodero, A. and Garcia, M.C., J. Qua. Spectroscopy & Rad. Tr., 198 (2017) 93.

[22] Sanghoo, P., Wonho, C., Se, Y.M. and Suk, J.Y., Adv. Phys. X, 4 (2019) 1526114.